Full Length Research Paper

Design of combined robust controller for a pneumatic servo actuator system with uncertainty

Samsul Bahari Mohd Noor, Hazem I. Ali* and Mohammad Hamiruce Marhaban

Department of Electrical and Electronic Engineering, Faculty of Engineering, University Putra Malaysia.

In this paper the position control design of a pneumatic servo actuator system using a combined H-inf /QFT technique is presented. First, an H-inf controller is designed to assure robust stability for the system. Particle swarm optimization (PSO) algorithm is used to tune the weighting functions. This method is used to find the optimal values of weighting functions parameters that lead to obtain an optimal H-inf-controller by minimizing the infinity norm of the transfer function of the nominal closed loop system. The quantitative feedback theory (QFT) is used to enhance the closed loop system performance. A multiplicative unstructured model extracted from the parametric uncertainty is used for control design. Finally, the simulation results are presented and compared with previous work.

INTRODUCTION

Robust control techniques such as modern H-inf and quantitative feedback theory (QFT) have received comparatively little attention in the fluid power literature, especially with regard to pneumatic systems (Karpenko and Sphri, 2004). The H-inf and QFT techniques are popular robust feedback control schemes that achieve desired system objectives in presence of plant and/or disturbance uncertainties. Recently, it has been esta-blished that both techniques (H-inf and QFT) can be used together to overcome each other's limitations (Nudeh and Farooq, 2007).

The H-inf optimization approach and its related approaches, being developed in the last two decades and still an active research area, it have been shown to be effective and efficient robust design methods for linear, time invariant control systems (Gu et al., 2005). It is one of the most known techniques available nowadays for robust control and the design of optimal controllers. Also, the H-inf control technique is an optimization method that takes into consideration a strong definition of the mathematical way to express the ability to include both classical and robust control concepts within a single design framework. It is an effective method for attenuating disturbances and noise that appear in the system (Alok, 2007). On the other hand, the design approach robust solutions may not give adequate transient response resulting in somewhat relaxed performance specifications (Nudeh and Farooq, 2007).

Quantitative feedback theory (QFT) is another control design in Nichols chart developed by Horowtz in early 1960. QFT is a unified theory that emphasizes the use of feedback for achieving the desired system performance tolerances despite plant uncertainty and plant disturbance.

QFT quantitatively formulates these factors in the form of the set of acceptable command or tracking input-output relationships and a set of possible plants that include the uncertainties (Jihong et al., 2007). It is generally understood that QFT achieves robust performance for minimum phase, stable and unstable plants that has limited success for non-minimum phase systems. Also, the output time response bounds sometimes do not entirely match with frequency domain bounds of system transfer functions (Nudeh and Farooq, 2007).

In this paper a combination of H-inf/QFT design technique for nonlinear and uncertain pneumatic servo actuator system is presented. This combination can give better performance than if only one of them is used. A simple and effective position controller of the system is

_____

*Corresponding author. E-mail: hazemcontrol2001@yahoo.com.
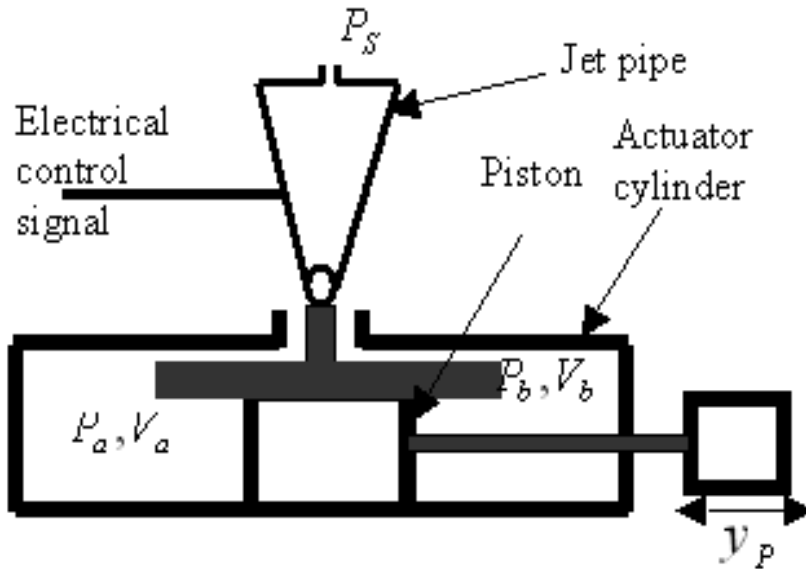
Figure 1. Schematic diagram of pneumatic servo actuator system.

the main objective of this paper. PSO method minimizes the cost function as a powerful optimization method with high efficiency in comparison to other methods. The use of PSO algorithm to tune the weighting functions simpl-fies the design procedure of the conventional controller.

PNEUMATIC SERVO ACTUATOR

System description

High performance position control of pneumatic actuators remains a difficult task. In most industrial applications, safety requires that the pressure of the air supply be kept low, which makes it difficult to design high bandwidth systems. Moreover, low supply pressure tends to limit the achievable actuator stiffness, which affects the ability of the servomechanism to reject disturbing loads. Nonlinear control valve flows and uncertainties in the plant parameters also complicate the design of high performance pneumatic servos. On the other hand, the pneumatic actuators are widely employed in position and speed control applications when cheap, clean, simple, and safe operating conditions are required. In recent years, low cost microprocessors and pneumatic com-ponents became available in the market, which made it possible to adopt more sophisticated control strategies in pneumatic system control (Jihong et al., 2007). The pneumatic cylinders can offer a better alternative to electrical or hydraulic actuators for certain types of applications and the pneumatic actuators provide the previously enumerated qualities at low cost. They are also suitable for clean environments and safer and easier to work with. However, position and force control of these actuators in applications that require high bandwidth is

difficult due to compressibility of air and highly nonlinear flow through pneumatic system components. A typical pneumatic system includes a force element (pneumatic cylinder), a command device (valve), connecting tubes, piston, pressure and force sensors. The external load consists of the mass of external mechanical elements connected to the piston and perhaps a force produced by environmental interaction (Edmond and Yildirim, 2001). A schematic diagram of the pneumatic actuator system is shown in Figure 1.

The purpose of the servo actuator unit is to move the load by displacement y_p in compliance with the com-manded signal. Figure 1 shows the schematic diagram of the electro-pneumatic servo actuator. The source of power used in this type of actuator is compressed air supplied to the jet pipe. An electromagnetic force generated by the flowing electric current rotates the jet pipe. Reacting to the pressure differential in the cylinder cavities, the piston together with the rod moves with speed dependent on the airflow, air pressure and load. The diameter and stroke of the piston are 80 and 50 mm, respectively. Output piston feedback is provided by a linear potentiometer, the slider of which is driven by the piston. The servo unit consists of a control surface actuator, a feedback transmitter, a polarized jet relay, and a power amplifier (Ali at al., 2008). The minor loop of the servo shown in Figure 2 is used to ensure a proportional movement with respect to input commands.

System model and dynamics

The analysis of pneumatic actuators requires a combination of thermodynamics, fluid dynamics and the
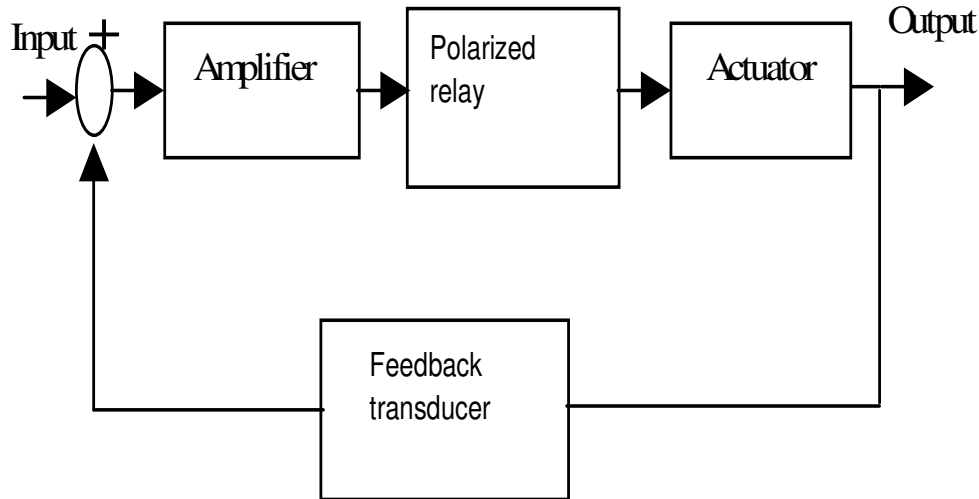
Figure 2. Block diagram of servo actuator system.

dynamics of motion. For constructing a mathematical model, three major considerations must be involved (Ali et al., 2009).

(i) The mass flow rates through the valve.
(ii) The pressure, volume and temperature of the air, in cylinder.
(iii) The dynamics of the load.

The valve is a four port pneumatic jet pipe valve. This valve is treated as equivalent to two three-port valves, one of each side of the cylinder. Considering the left hand side of the cylinder (Figure 1), the thermodynamic system is enclosed in the box, or control volume. Many studies have shown that for adequate models for controller design an isothermal behavior of the air may be assumed. Starting with the definition of the density, using the ideal gas equation and assuming an isothermal process the mass flow rates equations can be written as (Peter, 2010):

$$\dot{M}_a = \dot{\rho}_a V_a + \rho_a \dot{V}_a \tag{1}$$

$$-\dot{M}_b = \dot{\rho}_b V_b + \rho_b \dot{V}_b \tag{2}$$

where $\dot{M}_a$ and $\dot{M}_b$ are the mass flow rates in (chambers (a) and (b)) respectively, ρ is the density of the air, V_a and V_b are the volumes in chambers a and b.

For a symmetric cylinder the volumes in chambers a and b are given by:

$$V_a = V_o + A_P y_p \tag{3}$$

$$V_b = V_o - A_P y_p \tag{4}$$

where y_p is the position displacement, A_p is the piston area, V_o is the air volume in cylinder when the piston in mid point, V_a and V_b are the volumes in chambers a and b, respectively.

Differentiating Equations (3) and (4) and substitute them in (1) and (2) the following equations will be obtained:

$$\dot{M}_a = \frac{1}{\alpha R T_a} \dot{P}_a (V_o + A_P y) + \frac{1}{R T_a} P_a A_p \dot{y}_P \tag{5}$$

$$\dot{M}_b = \frac{1}{\alpha R T_b} \dot{P}_b (V_o - A_P y) + \frac{1}{R T_b} P_b (-A_p \dot{y}_P) \tag{6}$$

where R is the gas constant, α is the specific heat ratio, T_a and T_b are the temperatures in chambers a and b respectively, P_a and P_b are the pressures in chambers a and b respectively.

Rearranging the Equations (5) and (6) and adding the load dynamics equation that influences the overall performance of the piston motion, the system equations will be:

$$\dot{P}_a = \frac{\alpha R T_b}{(V_o + A_P y_P)} \dot{M}_a - \frac{\alpha P_a A_P}{(V_o + A_P y_P)} \dot{y}_P \tag{7}$$

$$\dot{P}_b = \frac{\alpha R T_b}{(V_o - A_P y_P)} \dot{M}_b + \frac{\alpha P_b A_P}{(V_o - A_P y_P)} \dot{y}_P \tag{8}$$

$$\ddot{y}_P = \frac{A_P}{M} P_a - \frac{A_P}{M} P_b - \frac{1}{M} F_L - \frac{1}{M} F_f \tag{9}$$

where M, F_L and F_f are the load mass, disturbing force and friction force respectively.

The equation that governs the mass flow rate of air through each control valve orifice is nonlinear equation and not suited for controller design. If a fast servo valve is used, the dynamics of the valve can be neglected. Assuming for the moment a positive input signal to the valve, a short line between valve and cylinder and chamber pressures of about half the supply pressure, the control valve equations will be simplified to be (Peter, 2010):

$$\dot{M}_a = K_V \frac{P_S}{2} u \tag{10}$$

$$\dot{M}_b = -K_V \frac{P_S}{2} u \tag{11}$$

where K_V is the valve coefficient, P_S is the supply pressure and u is the electric valve input signal respectively.

Substituting Equations (10) and (11) in Equations (7) and (8) and combining the Laplace transformations of Equations (7), (8) and (9) allows the operating point dependant transfer function model of the open loop system to be written as:

$$y_P(s) = G_p(s)U(s) - G_d(s)F_d(s) \tag{12}$$

where

$$G_p(s) = \frac{2K\dfrac{\alpha RTA_P}{MV_o}}{s(s^2 + \dfrac{f}{M}s + \dfrac{2\alpha(A_P)^2 P_i}{MV_0})} \tag{13}$$

and

$$G_d(s) = \frac{\dfrac{1}{M}}{s(s^2 + \dfrac{f}{M}s + \dfrac{2\alpha(A_P)^2 P_i}{MV_0})} \tag{14}$$

where $K = K_V \dfrac{P_S}{2}$

This system considered, a four-port valve used to control a double acting through rod cylinder. There are three nonlinearities in the pneumatic servo system. The first one is the nonlinear characteristic of the valve, and the other two nonlinearities are the volume and bulk modulus

when they are used as coefficients in the equations. The nominal values of system parameters are given in Table 1 (Ali et al., 2008).

The frequency characteristics of the pneumatic actuator with all parameters uncertainty and with a wide range of load variation from 0.1 to 100 kg are shown in Figure 3. These characteristics show that the system bandwidth decreases when the load increases, until the system becomes slower. Also the phase margin decreases when the load increases and this tends the system to oscillate and be unstable system.

CONTROLLER DESIGN

The design requirements and objectives for pneumatic servo actuator system in this paper is to find a linear, output feedback control $u(s) = K_\infty(s)y(s)$ which ensures that the closed loop system will be internally stable. Also, the required closed loop system performance should be achieved for the nominal plant G_p.

Since the system model has jw-axis pole, the H_∞ controller, if it is reliably computed, would have marginally stable closed loop pole at the corresponding jw-axis location. This problem lead to singularities in the equations that determine the state space realization of H_∞ control law. So a simple bilinear transform has been found to be extremely useful when it used with robust control synthesis. This transformation can be formulated as a jw-axis pole shifting transformation (Chiang and Safanov, 1997):

$$s = \frac{\hat{s} + p_1}{\dfrac{\hat{s}}{p_2} + 1} \tag{15}$$

where $p_1 < 0$ and selected to be 0.1, p_2 is selected to be infinity.

This is equivalent to simply shifting the jw-axis by p_1 units to the left. The H_∞ controller is obtained for the shifted system then it is shifted back to the right with the same units.

Weighting functions selection

One of the important parts in the design of H_∞ controller is the selection of weighting functions and weighting gains for specific design problem. This is not an easy procedure and often needs many iterations and fine-tuning and it is hard to find general formula for the weighting functions that will work in every case (Anselmo and Moura, 1998). So to obtain a good control design, it

Table 1. The nominal system model parameters and their range.

Uncertain parameter	Minimum value	Nominal value	Maximum value
Piston area, A_P (m^2)		0.005	
Air density, $\rho(\dfrac{kg}{m^3})$		1.185	
Ideal gas constant, R $(\dfrac{J}{kg.K})$		287	
Air volume when the piston in mid point, V_o $(m^3) \times 10^4$	1.5	2.5	4
Chamber pressure, P_i (bars)		3	4
Load mass M (Kg)	0.1	1	100
Viscous damping coefficient, f $(\dfrac{N.\sec}{m})$	50	60	80
Overall valve gain, $K(\dfrac{kg}{s.V}) \times 10^3$	3.2	3.4	
Temperature of air source, T (K°)		293.15	
Specific heat ratio, α		1.4	
Potentiometer constant, K_P (V/m)		400	

is necessary to select suitable weighting functions. The performance and control weighting functions formulas used in this paper are (Chiang and Safanov, 1997; Zhou and Doyle, 1998):

$$W_p(s) = \frac{\beta(as^2 + 2\zeta_1 w_c \sqrt{a}s + w_c{}^2)}{(\beta s^2 + 2\zeta_2 w_c \sqrt{\beta}s + w_c{}^2)} \qquad (16)$$

$$W_u(s) = \frac{s^2 + 2\dfrac{w_{bc}}{\sqrt{M_u}}s + \dfrac{w^2{}_{bc}}{M_u}}{\varepsilon s^2 + 2\sqrt{\varepsilon}w_{bc}s + w^2{}_{bc}} \qquad (17)$$

where β is the d.c. gain of the function which controls

the disturbance rejection, a is the high frequency gain which controls the response peak overshoot, w_c is the function crossover frequency, ζ_1 and ζ_2 are the damping ratios of crossover frequency, w_{bc} is the controller bandwidth, M_u is the magnitude of $K_\infty S$, and ε is a small value.

H_∞ Controller design

The H_∞ control design deals with both structured and unstructured uncertainty. However, since a design scheme involving unstructured uncertainty gives more control over the system (as it can cover unmodeled

Bode diagram
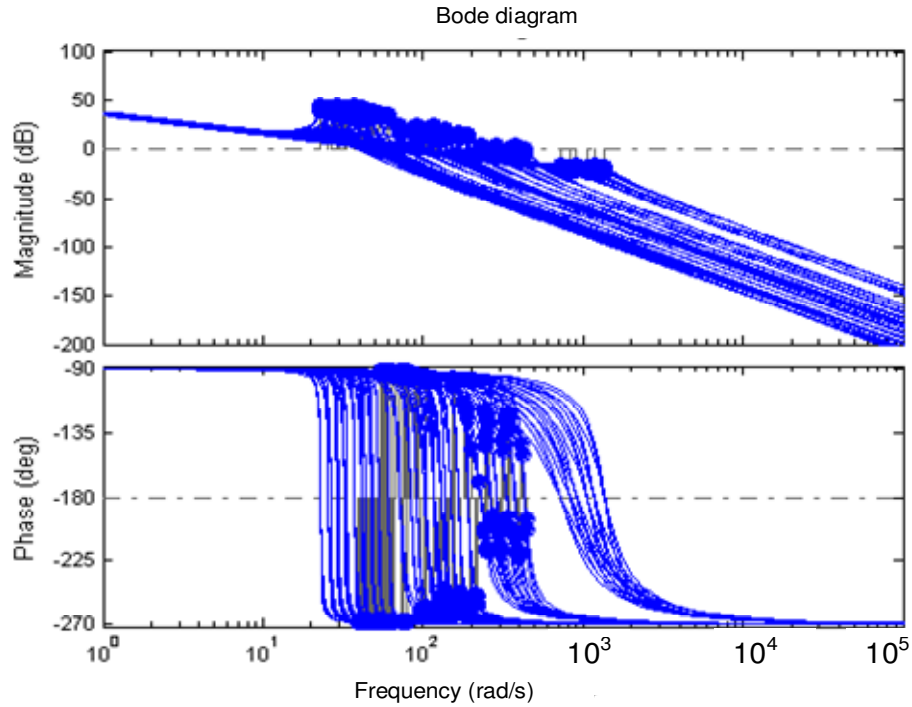
Figure 3. Frequency response characteristics of the system with parameters uncertainty and with M=0.1 to 100 kg.

dynamics at high frequencies (Nudeh and Farooq, 2007)), the plant with structured uncertainty can be expressed in terms of unstructured multiplicative uncertainty. By selecting a set of nominal plants to evaluate the disk of uncertainty, the uncertainty plant is:

$$G_p \text{ is the } \hat{G}_p = G_p(1 + W_m \Delta_m) \qquad (18)$$

where nominal plant and the multiplicative uncertainty Δ_m can be expressed as:

$$\Delta_m = \frac{\hat{G}_p - G_p}{G_p} \qquad (19)$$

From Equation (19), multiplicative uncertainty weight W_m can be calculated such that $|\Delta_m(jw)| \le |W_m(jw)|$ and can be expressed as:

$$W_{m1}(s) = \frac{-0.3917s^4 + 0.1147s^3 - 153680s^2 + 1.978 \times 10^6 s - 6.056 \times 10^9}{s^4 + 10.28s^3 + 416300s^2 - 1.496 \times 10^6 s + 1.538 \times 10^{10}} \qquad (20)$$

$$W_{m2}(s) = \frac{-0.9989s^4 + 1.06 \times 10^{-7} s^3 - 13020s^2 - 1261s - 295200}{s^4 + 0.5313s^3 + 14520s^2 + 8203s + 2.262 \times 10^7} \qquad (21)$$

The H_∞ controller has been designed so that the infinity norm from input $W = \begin{bmatrix} y_d \\ F_d \end{bmatrix}$ to output $Z = \begin{bmatrix} e_p \\ e_u \end{bmatrix}$ is minimized.

where y_d is the set point and F_d is the input disturbance, e_p, e_u are the weighted error and control signals.

Figure 4 shows the standard feedback diagram of the system with weights. The generalized plant P is expressed by:

$$P = \begin{bmatrix} 0 & 0 & 0 & W_m G_p \\ -W_p & W_p & W_p G_d & -W_p G_p \\ 0 & 0 & 0 & W_u \\ -1 & 1 & G_d & -G_p \end{bmatrix} \qquad (22)$$

The lower linear fractional transformation of the generalized plant P and controller K_∞ can be described by:

$$F_l(P, K_\infty) = P_{11} + P_{12} K_\infty (1 - P_{22} K_\infty)^{-1} P_{21} = N \qquad (23)$$

and

Figure 4. The standard feedback diagram of the system with weights.

$$N = \begin{bmatrix} -W_m T & W_m T & W_m G_d T \\ -W_p S & -W_p S & W_p G_d S \\ -W_u K_\infty S & W_u K_\infty S & W_u G_d K_\infty S \end{bmatrix} \quad (24)$$

where $S = (1 + G_p K_\infty)^{-1}$ is the sensitivity function of the nominal plant and $T = G_p K_\infty (1 + G_p K_\infty)^{-1}$ is the complementary sensitivity function.

The objective of H_∞ control is to find the controller K_∞ that internally stabilizes the system such that the maximum singular value of N is minimized.

On the other hand, the H_∞ control minimization depends on γ-iteration (Skogestad and Postlethwaite, 2005) to find the stabilizing controller such that:

$$\|N\|_\infty < \gamma \quad (25)$$

In this paper the optimal value of γ was found by using PSO algorithm. This can be achieved by tuning the weighting functions that have a significant effect on the overall design of H_∞ control technique. The optimal value of γ is the infimum overall γ such that the H_∞ control conditions in (Zhou and Doyle, 1998) are satisfied.

Combined controller design

To combine both H_∞ and QFT control techniques, the following steps must be ensured:

(i) The upper and lower tracking performance specifications must be satisfied as:

$$|T_L(jw)| \le \left| \frac{F(jw)K(jw)\hat{G}_p(jw)}{1 + L(jw)} \right| \le |T_U(jw)| \quad (26)$$

where $T_L(jw)$ and $T_U(jw)$ are the closed loop tracking bounds, F(jw) is the prefilter and $\hat{G}_p(jw)$ is the uncertain plant. An acceptable response must lie between the upper and lower bounds of the tracking performance specifications (Fujita et al., 2008). These closed loop-tracking bounds $T_L(s)$ and $T_U(s)$ are selected to give a closed loop bandwidth between 3.88 rad/s and 11 rad/s in case of a small range of load variation and between 1.41 rad/s and 4.47 rad/s in case of a wide range of load variation. The tracking bounds used in the design of the controller for small and wide ranges of load variation, respectively, are:

$$T_{Ls}(s) = \frac{4 \times 10^5}{(s+4)(s+20)(s+50)(s+100)} \quad (27)$$

$$T_{Us}(s) = \frac{800(s+5)}{(s^2+10s+40)(s+100)} \quad (28)$$

$$T_{Lw}(s) = \frac{3600}{(s+2.3)(s+2.127)(s^2+166.1s+7359)} \quad (29)$$

$$T_{Uw}(s) = \frac{213.4454(s+5.95)}{(s^2+4.399s+12.05)(s+105.4)} \quad (30)$$

In case of a small range of load variation, the time response specification of $T_{Ls}(s)$ is overdamped and has a rise time of 0.662 s and settling time of 1.06 s for 2%

Figure 5. Block diagram of the two degrees of freedom combined H_∞/QFT controller for pneumatic servo actuator system.

criterion. $T_{Us}(s)$ has a rise time of 0.194 s, settling time of 0.778 s for 2% criterion and 10% maximum overshoot. Whereas, in case of a wide range of load variation, the time response specification of $T_{Lw}(s)$ is overdamped and has a rise time of 1.78 s and settling time of 2.67 s for 2% criterion. $T_{Uw}(s)$ has a rise time of 0.507 *s*, settling time of 1.52 s for 2% criterion and 10% maximum overshoot.

This requirement is achieved using H_∞-norm optimasation algorithm by minimizing the following performance criterion (objective function) in Equation (25) such that:

$$\delta_L(jw_i) \leq \delta_R(jw_i) \tag{31}$$

where

$$\delta_L(jw_i) = \left| \frac{K(jw_i)\hat{G}_p(jw_i)}{1 + K(jw_i)\hat{G}_p(w_i)} \right| - \left| \frac{K(jw_i)G_p(jw_i)}{1 + K(jw_i)G_p(jw_i)} \right| \tag{32}$$

$$\delta_R(jw_i) = |T_U(jw_i)| - |T_L(jw_i)| \tag{33}$$

(ii) In order to fit the feedback closed loop gain of the system inside the upper and lower boundaries, the prefilter F(jw) is designed.

The control design technique can be formulated as two degrees of freedom QFT control strategy as shown in Figure 5. In this method the designed controller K(s) is the resulting controller from H_∞-norm optimisation algorithm. The PSO algorithm was used to tune the weighting functions to obtain the optimal values of their

parameters to ensure a controlled system with a good disturbance rejection, good transient response and low control signal. The flowchart of combined H_∞/QFT control design procedure is shown in Figure 6. The cost function used in PSO algorithm for tuning the weighting functions is the performance criteria in Equation (25). The algorithm obtains the minimum value of the infinity norm of the performance criteria that achieves the QFT constraint in Equation (31). The minimization process of the objective function in Equation (25) represents the reduction of the variation of the closed loop responses due to the uncertainty in the system, the reduction of the peak magnitude, the reduction of the sensitivity function which is required to improve the response due to the disturbing force and finally the reduction of the control effort.

Since the controller K(s) in the combined H_∞/QFT design is obtained by H_∞-norm, the following steps are not needed:

(i) Generating the uncertain plant templates bounds on the Nichols chart procedure.
(ii) The loop shaping step of the nominal L(jw), which is performed manually and depends on the experience of the designer.

The time consumed by the above two steps is saved in the design of combined H_∞/QFT controller.

The PSO algorithm is used to tune the selected weighting functions to obtain the optimal values of their parameters that ensure a controlled system with a good disturbance rejection, good transient response and low
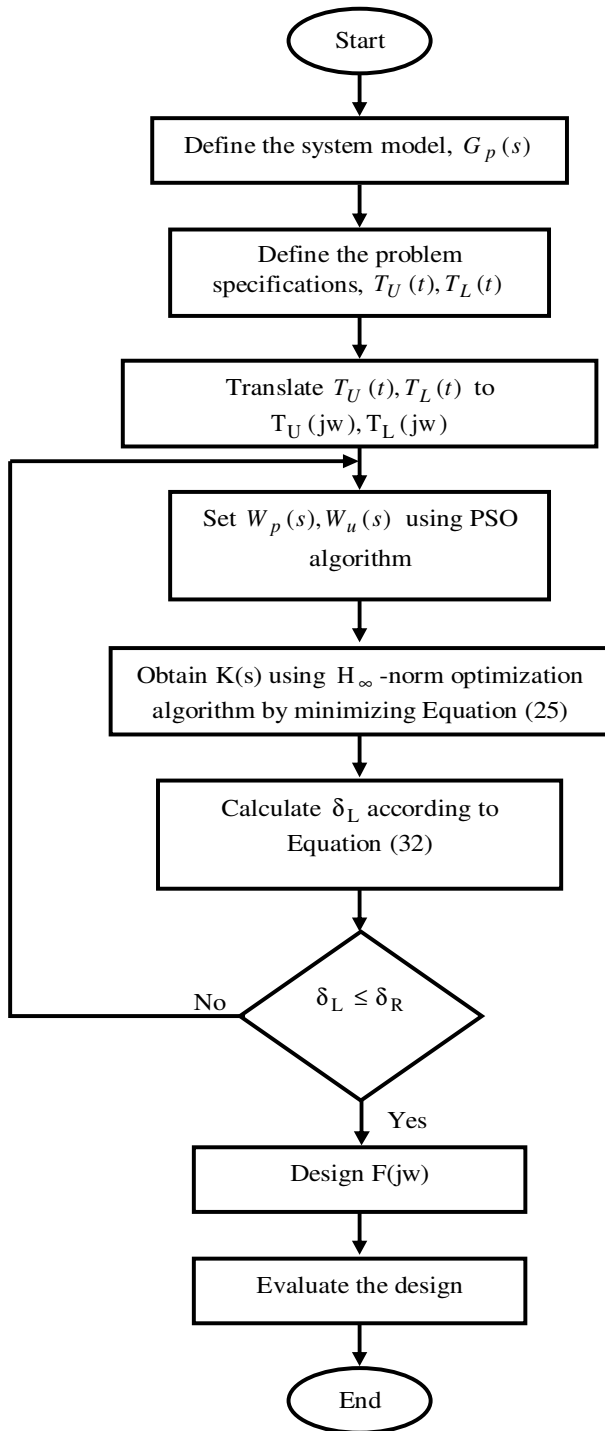
$$v_i^{k+1} = h \times v_i^k + c_1 \times rand \times (x_i^b - x_i^k) + c_2 \times rand \times (x_i^g - x_i^k)$$
(34)

$$x_i^{k+1} = x_i^k + v_i^{k+1}$$
(35)

where v_i^k is the particle velocity, x_i^k is the current particle position, w is the inertia weight and it is selected to be 1.5, x_i^b and x_i^g are the best value and the global best value, rand is a random function between 0 and 1, c_1 and c_2 are learning factors and are selected to be $c_1 = c_2 = 2$. The swarm size is (100) with (7-dimensions) (variables to be obtained) and the number of generations is (100). The proposed PSO algorithm can be described by the flowchart shown in Figure 7.

It was found that setting the parameters of PSO to: population size equal to 10, inertia weight factor $h = 2$, $c_1 = 2$ and $c_2 = 2$, maximum iteration set to 100 were sufficient to produce the best parameters of the weighting functions that give the minimum value of Equation (25) and achieves the QFT requirement in equation (31).

In the following, the PSO steps for obtaining the optimal parameters of the performance and control weighting functions are done by minimizing Equation (25) such that Equation (31) is satisfied.

Step 1: Define the system model $G_p(s)$.

Step 2: Initialize the individuals of the population randomly in the search space. These individuals represent the parameters of the weighting functions $(W_u(s), W_p(s))$.

Step 3: Construct the overall augmented plant, P.

Step 4: For each initial η_i of the population, where η_i is the vector of the parameters to be optimized in each case of the proposed controllers and i=1,...., n, where n denotes the population size of PSO, determine the cost function N in Equation (25) using the built in function in Matlab Software.

Step 5: Compare each value of equation (25) with its personal best x_i. The best value among the x_i is denoted as x_i^g.

Step 6: Update the velocity of each individual η_i according to (34).

Step 7: Update the position of each individual η_i according to (35).

Step 8: If the number of iterations reaches the maximum, then go to step 9, otherwise, go to step 4.

Step 9: If $\delta_L(jw_i) \le \delta_R(jw_i)$ then go to 10, otherwise, go to step 2.

Figure 6. Flowchart of combined H_∞ /QFT control design procedure.

control signal. The cost function used in PSO algorithm is the performance criteria in Equation (25). The algorithm obtains the minimum value of the infinity norm of the performance criteria. The velocity and position equations of PSO algorithm are (Zheng et al., 2007; Siby et al., 2010):
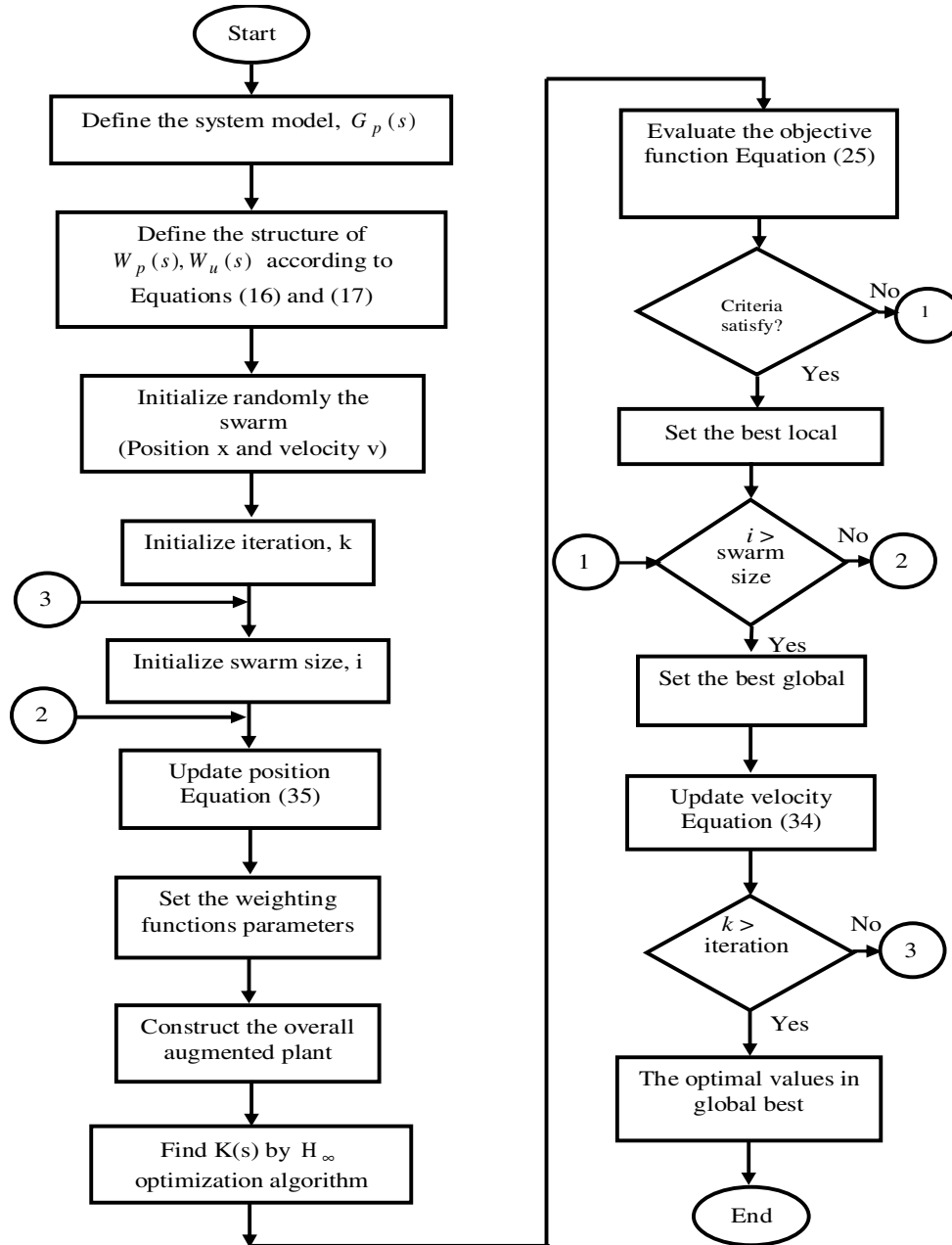
Figure 7. Flowchart of PSO algorithm for determining weighting functions parameters.

Step 10: The latest x_i^g is the optimal controller parameter.

The following designed combined H_∞/QFT controllers for small and wide ranges of load variation, respectively:

$$K_s(s) = \frac{0.04935s^2 + 49.36s + 1.234 \times 10^5}{s^3 + 193.5s^2 + 1.266 \times 10^4 s + 4.515 \times 10^5} \quad (36)$$

$$F_s(s) = \frac{0.07s + 1}{3 \times 10^{-5} s^2 + 0.1481s + 1} \quad (37)$$

$$K_w(s) = \frac{0.0003002s^4 + 0.06373s^3 + 30.96s^2 + 388s + 1.55 \times 10^4}{s^5 + 32.33s^4 + 1342s^3 + 1.236 \times 10^4 s^2 + 1.239 \times 10^5 s + 4.462 \times 10^5} \quad (38)$$

$$F_w(s) = \frac{0.5s + 1}{10^{-6} s^2 + 0.6s + 1} \quad (39)$$

The weighting functions optimal parameters obtained using PSO algorithm for the two designed controllers are given in Table 2.

Table 2. Optimal parameters of weighting functions.

Load range/parameter	β	α	w_c	ζ_1	ζ_2	w_{bc}	M_u
Load (M)=0.1 to 5 Kg	100	2.8×10^{-2}	12.5	1.8	4.96	50	15
Load (M)=0.1 to 100 Kg	3.5725	1.3×10^{-2}	4.94	1.38	16.1242	10.01	11.001
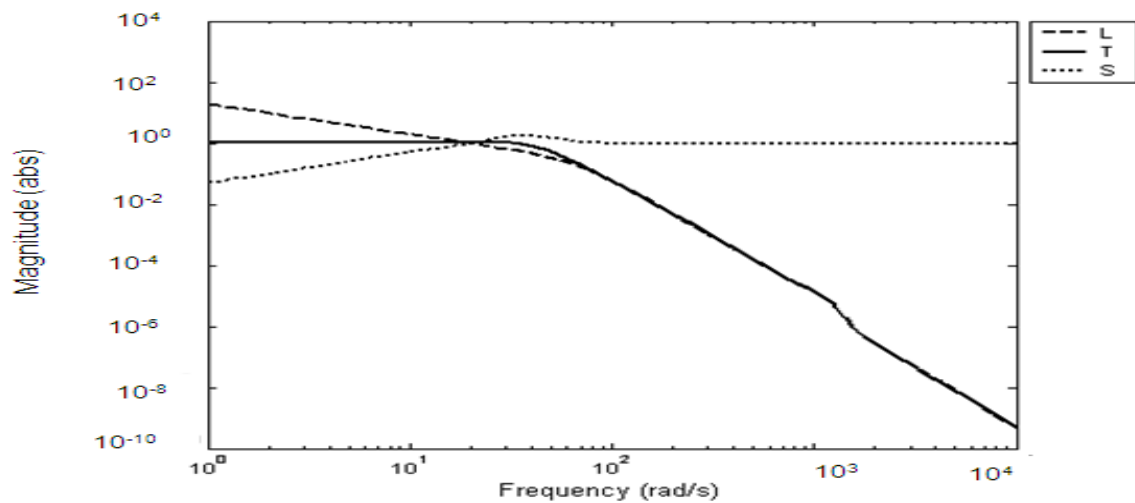
(a) M=0.1 to 5 Kg
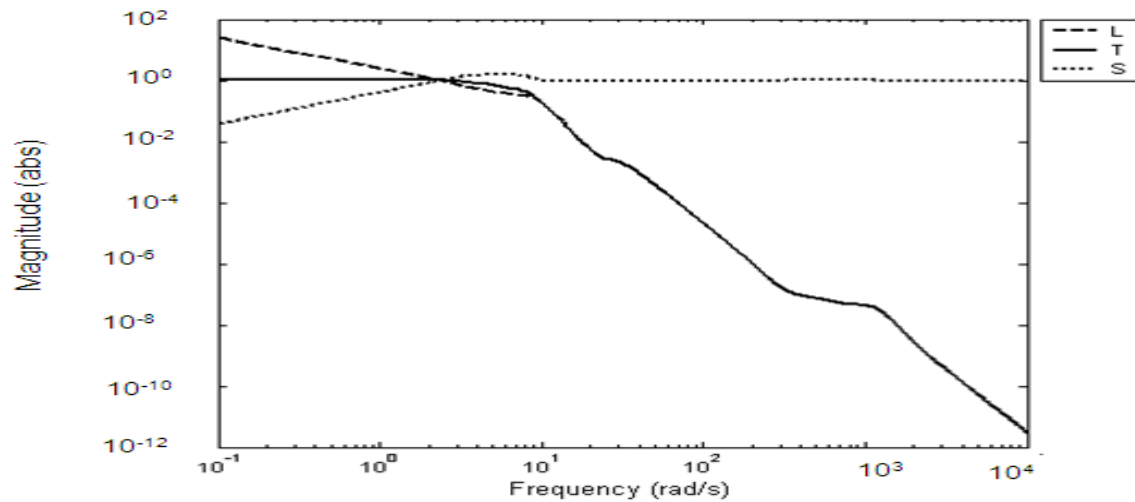
(b) M=0.1 to 100 Kg

Figure 8. Frequency characteristics plot of complementary sensitivity T, sensitivity S and nominal loop L.

RESULTS AND DISCUSSION

A frequency characteristics plot of complementary sensitivity function T, sensitivity function S and nominal loop L are shown in Figure 8. On the other hand, it depends on the actuator load variation; two cases of load variation ranges have been used. The first case is the small range of load variation with load variation from 0.1 to 5 kg. The second case is the wide range of load variation with load variation from 0.1 to 100 kg. These two cases have been classified for the purpose of comparison with previous work that used small range of load variation. Figure 9 shows the singular value of the controlled closed loop system. It seen that the maximum value of the closed loop system with the two cases of load variation is less than one. This means that the condition of the
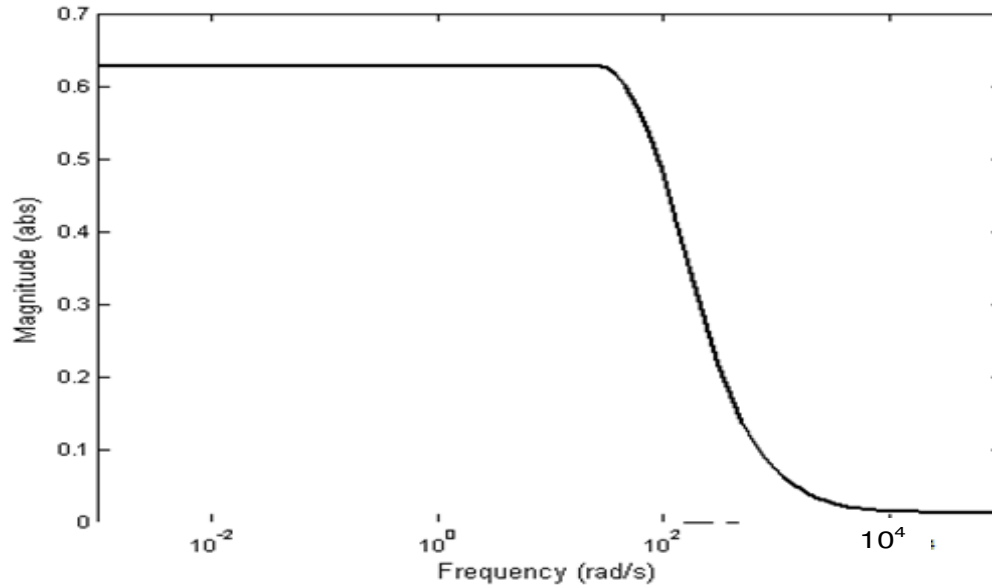
(a) M=0.1 to 5 Kg
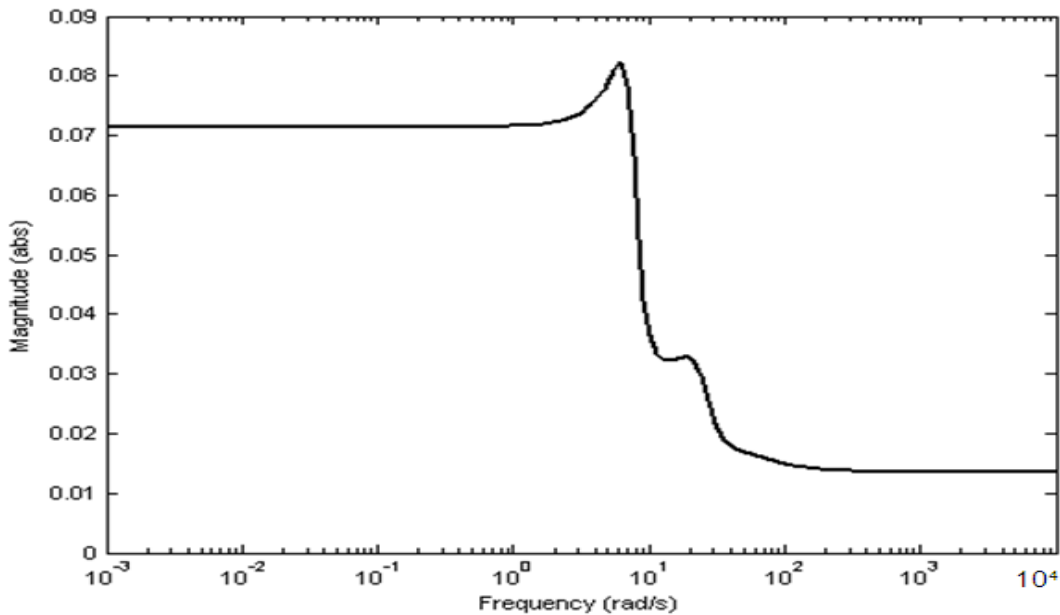
(b) M=0.1 to 100 Kg

Figure 9. The largest singular value of the closed loop controlled system.

performance criteria is satisfied. A frequency characteristic of the sensitivity function compared with the inverse of the performance weighting function W_p is shown in Figure 10. It is clear that the magnitude of the sensitivity function is less than the inverse of the performance weighting function for all frequencies. Figure 11 shows the frequency response of the controlled system with all parameters uncertainty. It is shown that

the system is stable with all parameters uncertainty; this means the robust stability of the system has been achieved. The step response characteristics of the nominal system and uncertain system can be shown in Figure 12. The response characteristic of the uncertain system with combined H_∞/QFT controller is shown in Figure 13. It is clear that the performance of the system has been improved and the response lies between upper
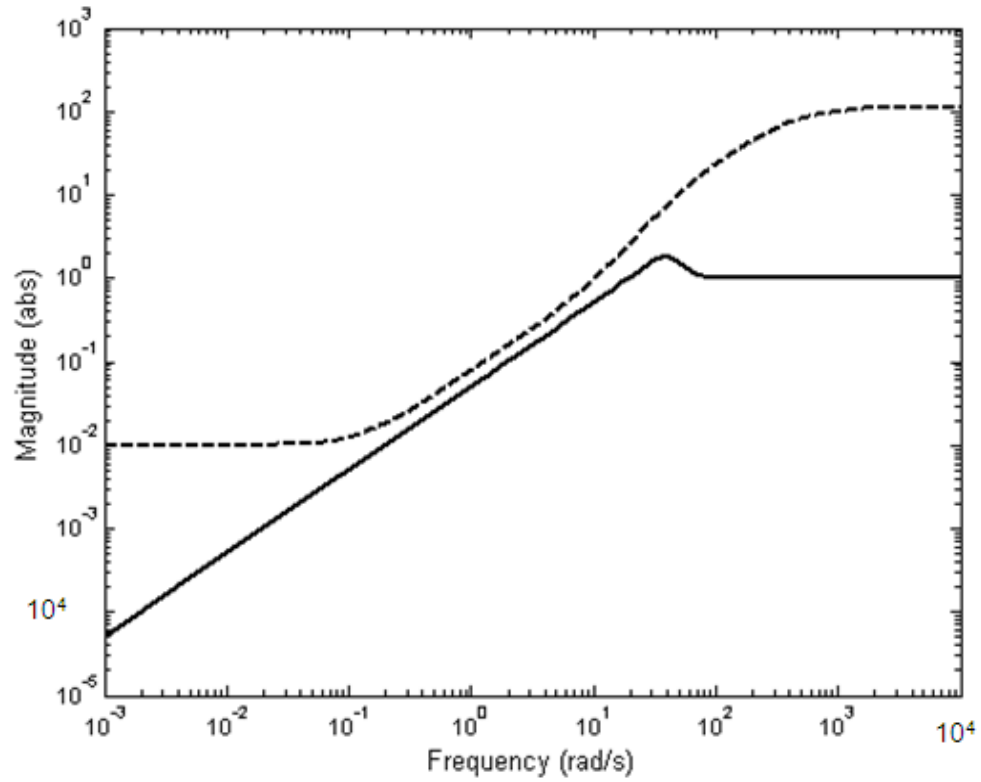
(a) M=0.1 to 5 Kg
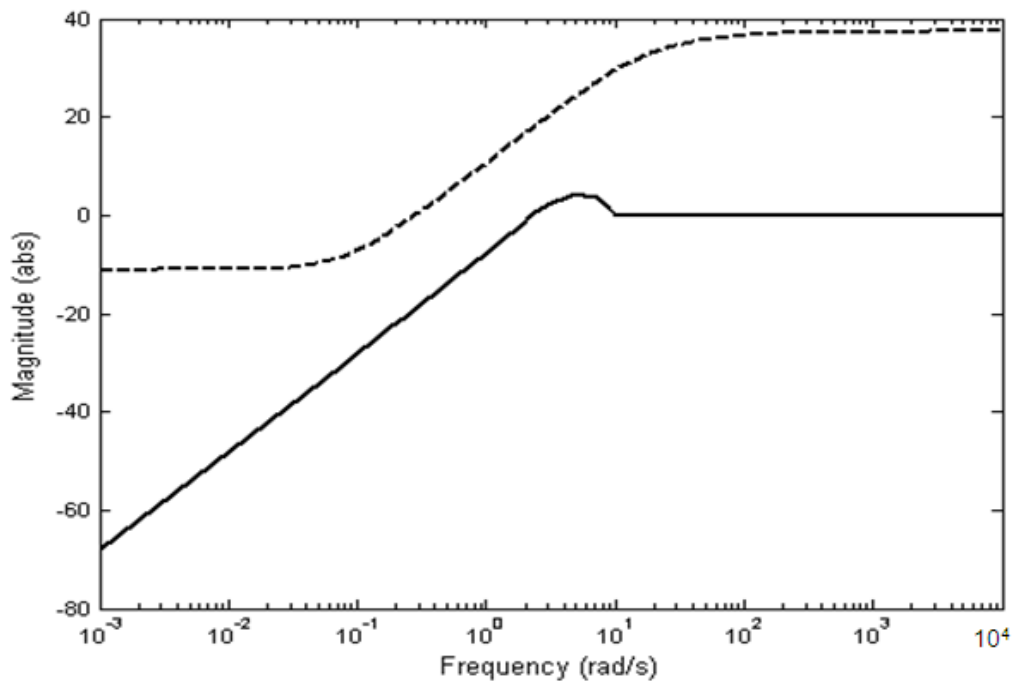
(b) M=0.1 to 100 Kg

Figure 10. Frequency characteristics plot of sensitivity S (solid line) and inverse of weighting function W_p (dotted line).
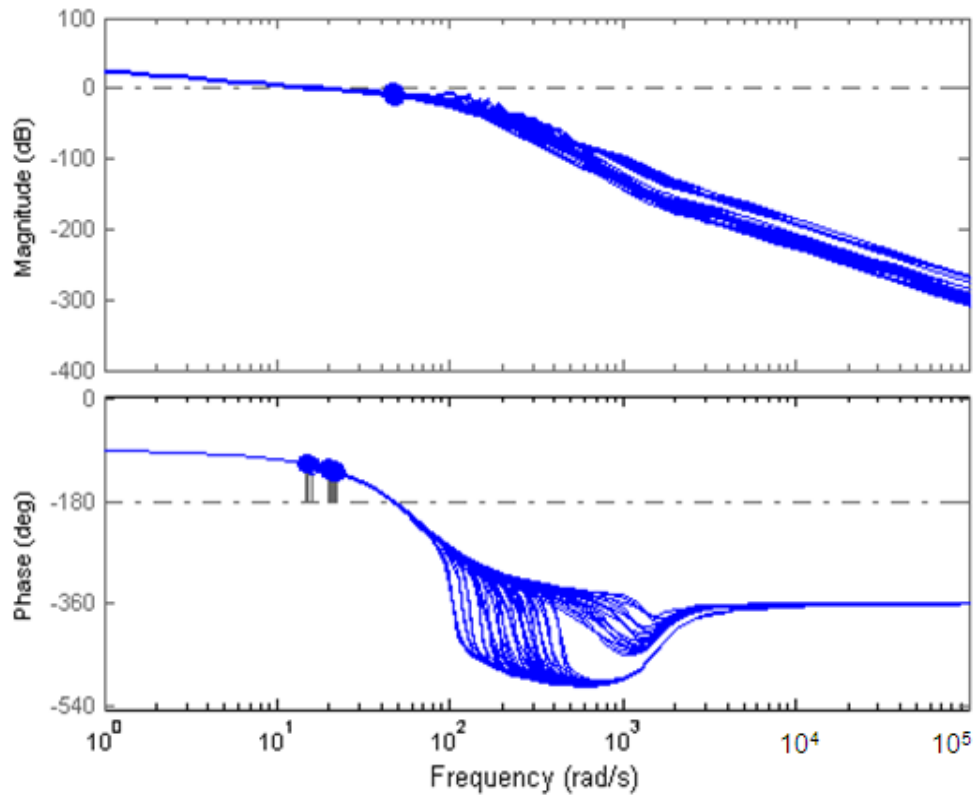
(a) M=0.1 to 5 Kg
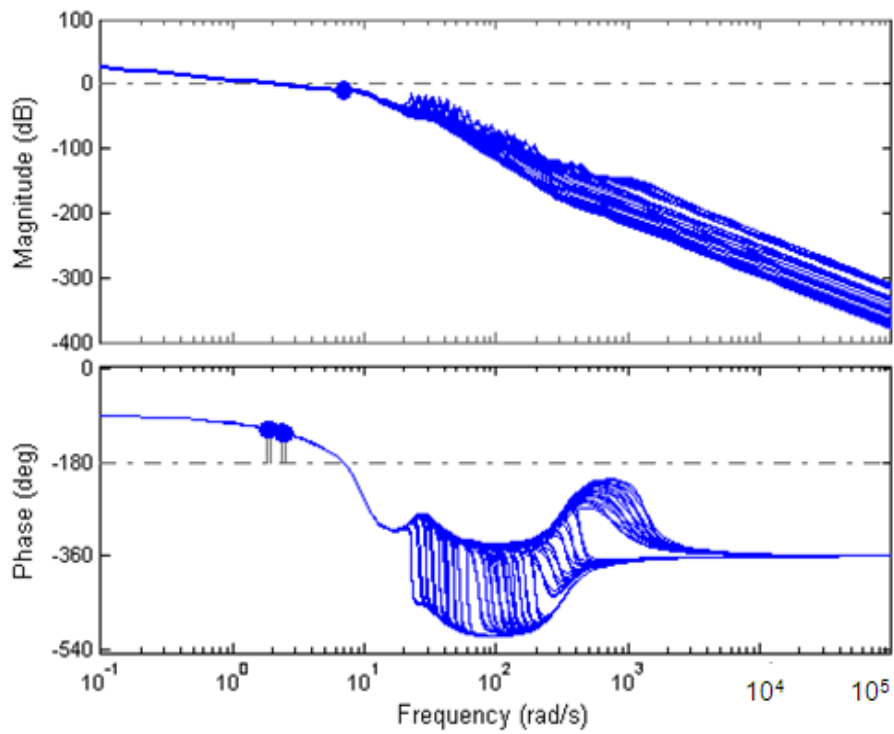
(b) M=0.1 to 100 Kg

Figure 11. Frequency response characteristics of the system with H_∞ controller.
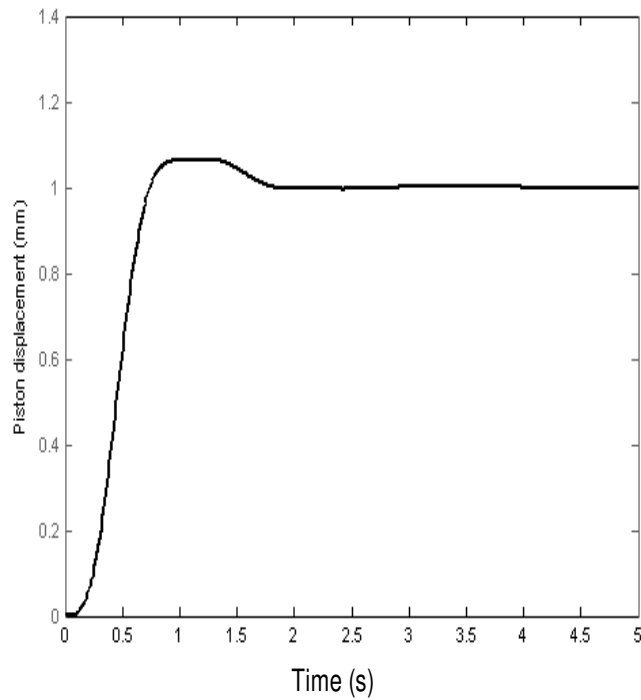
(c) Nominal plant with M=0.1 to 100 Kg
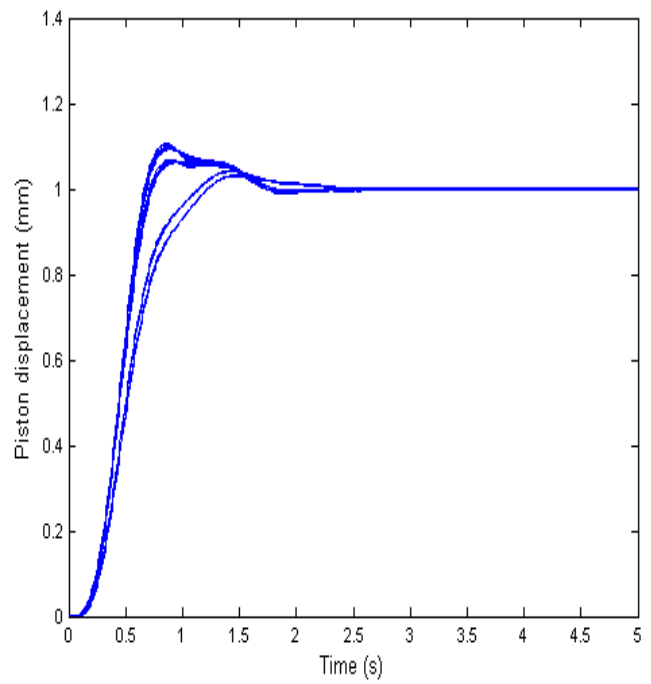
(d) Perturbed plant with M=0.1 to 100 Kg

Figure 12. Step response of the system with H_∞ controller.
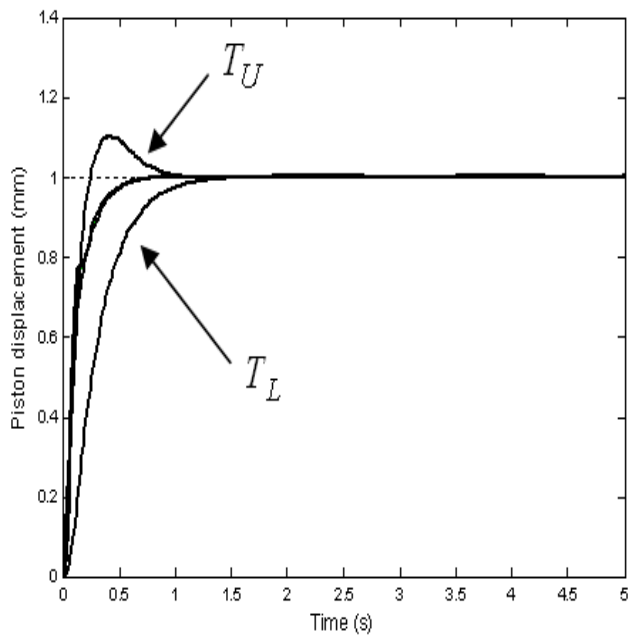
(a) M=0.1 to 5 Kg
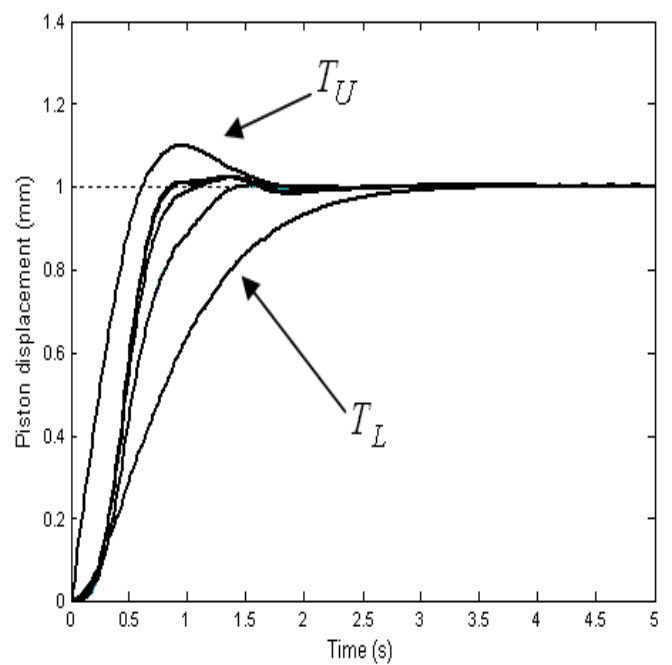
(b) M=0.1 to 100 Kg

Figure 13. Step response of the perturbed system with combined H_∞ /QFT.
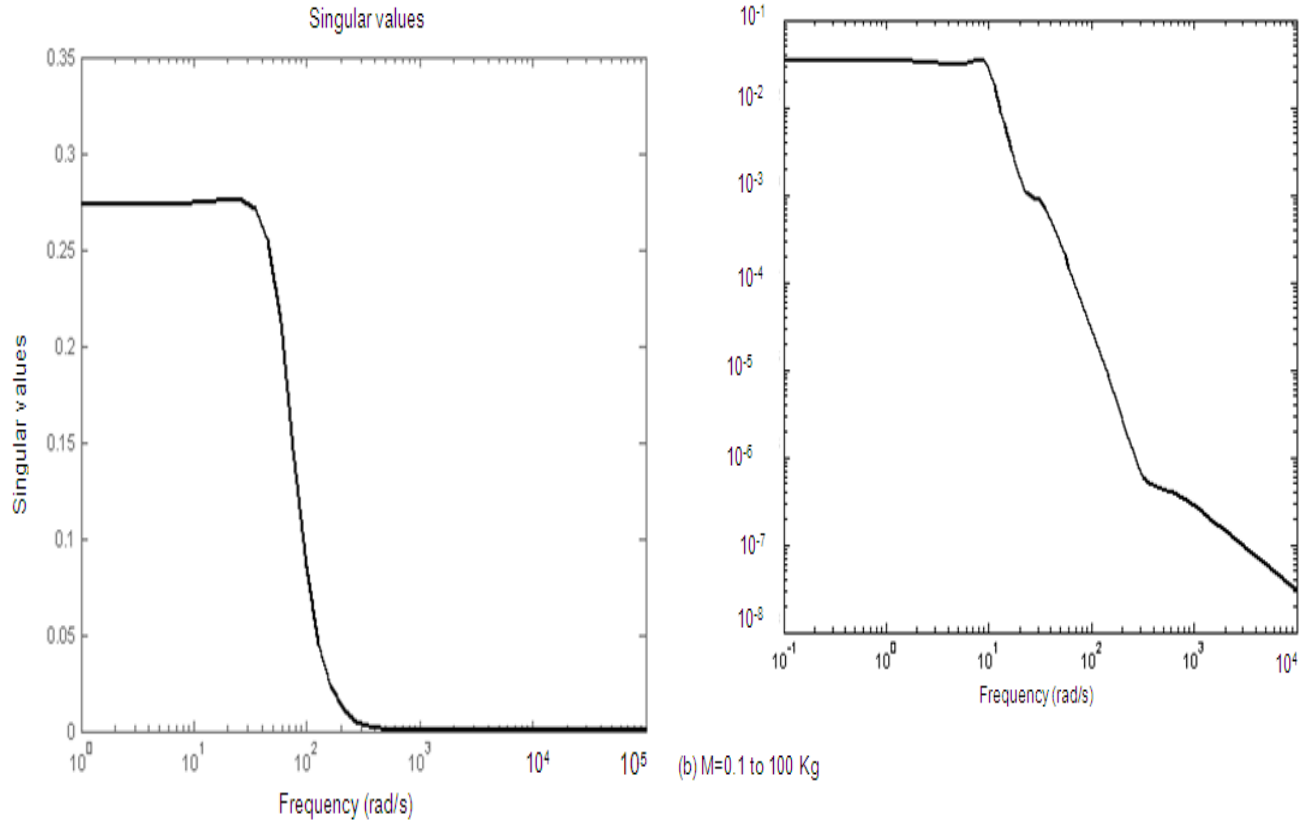
(a) M=0.1 to 5 Kg

(b) M=0.1 to 100 Kg

Figure 14. The largest singular value of the control signal.

Table 3. Comparison between QFT controller and combined H_∞/QFT controller for pneumatic servo actuator system.

Controller	Small range of load variation		Wide range of load variation	
Specifications	Standard QFT controller	Hybrid H_∞/QFT controller	Standard QFT controller	Hybrid H_∞/QFT controller
Rise time, t_r (s)	0.661	0.292	1.49	1.03
Settling time (2%), t_s (s)	1.06	0.533	2	1.3
Overshoot, $\%M_p$	-	-	-	3
GM (dB)	5.16	6.35	3.2	9.4
PM (degree)	30.8	53.2	57	55.7
Controller order	4	3	5	5

and lower boundaries. As one of the necessary practical requirements a small magnitude of control signal has been obtained as shown in Figure 14. Table 3 compares the results of the time and frequency responses of the standard QFT controller and combined H_∞/QFT controller for pneumatic servo actuator system. It is shown that, the design of the combined H_∞/QFT controller is

more efficient for the pneumatic servo actuator system than the standard QFT controller. In case of small range of load variation, it can be seen that the time and frequency response specifications obtained by the combined H_∞/QFT controller are better than those obtained by standard QFT controller. Furthermore, the resulting controller is lower than the standard QFT controller. On

the other hand, in case of wide range of load variation, it can be seen that the rise time, settling time and gain margin obtained by the combined H_∞/QFT controller are better than those obtained by standard QFT controller.

Conclusions

A robust combined H_∞/QFT controller has been designed to assure robust stability and robust performance of the uncertain pneumatic servo actuator system with small and wide ranges of load variation. First, the H_∞ controller was designed to achieve robust stability of the system. The parametric structured uncertainty of the system was converted to multiplicative unstructured uncertainty.

Suitable formulas for performance and control weighting functions were selected for controller design requirements. The particle swarm optimization algorithm (PSO) has been used to tune the selected performance and control weighting functions by minimizing the infinity norm of the transfer function of the nominal closed loop system. PSO method was used because of its simplicity and easy to implement. The obtained weighting functions have been used to obtain the optimal robust controller that achieves the position control of the pneumatic servo actuator system.

To enhance the closed loop system performance the prefilter was designed to fit the closed loop system in the set inside the upper and lower bounds. The design of combined H_∞/QFT controller has achieved in the same time the design requirements that arise from both QFT and H_∞ control techniques. Finally, the combined H_∞/QFT controller has been given better performance than the previous works that used only one of them. The robust stability and performance of the proposed design were verified by simulation.

REFERENCES

Ali HI, Mohd Noor SB, Bashi SM, Marhaban MH (2008). Robust QFT controller design for positioning a pneumatic servo actuator, Proceeding of student conference on res. Dev., Johor, Malay., 128:1-4.

Ali HI, Mohd Noor SB, Bashi SM, Marhaban MH (2009). A review of pneumatic actuators (modeling and control), Aus. J. Basic Appl. Sci., 3(2): 440-454.

Alok S (2007). Linear systems optimal and robust control, Taylor and Francis Group, USA.

Anselmo B, Moura SR (1998). H_2 and H_∞ control for Maglev vehicles, IEEE Control Syst., 18: 18-25.

Chiang RY, Safonov MG (1997). Matlab robust control toolbox, Mathworks, Inc., USA.

Edmond R, Yildirim H (2001). A high performance pneumatic force actuator system, ASME, J. Dyn. Syst. Measur. Control., 122(3): 416-425.

Fujita T, Kawashima K, Miyajima T (2008). Effect of servo valve dynamic on precise position control of a pneumatic servo table, Int. J. Autom. Technol., 2(1): 43-48.

Gu D W, Petkov P, Konstantinov M (2005). Robust control design with Matlab, Springer.

Jihong W, Ulle K, Jia K (2007). Tracking control of nonlinear pneumatic actuator systems using static state feedback linearization of the input-output map, Proceedings Estonian Acad. Sci. Phys. Math., pp. 47-66.

Karpenko M, Sephri N (2004). QFT design of a PI controller with dynamic pressure feedback for positioning a pneumatic actuator, Proceeding of of American control conference, Boston, Nassachusetts, pp. 5084-5089.

Peter B (2010). Pneumatic drives system design, modeling and control, Springer, Verlag Berlin Heidelberg.

Siby A, Sugata S, Mukund S (2010). Particle swarm optimization based diphanting equation, Int. J. Bio-Inspired Comput., 2 (2): 100-114.

Zheng S F, Hu S L, Su S X, Lin C F, Lai X W (2007). A modified particle swarm optimization algorithm and application, Proceedings of the sixth int. conf. mach. learning cybernet. Hong Kong, 945-951.

Zhou K, Doyle J C (1998). Essentials of robust control, Prentice Hall.